Medical Engineering and Physics 111 (2023) 103932

Contents lists available at ScienceDirect

Medical Engineering and Physics

journal homepage: www.elsevier.com/locate/medengphy

Development and validation of an algorithm to determine the minimal factors needed for non-invasive measurement of the in vivo primary stability of cementless hip implants

Carlos A. Fonseca Ulloa [a,*], Anja Seeger [a], Frederike S. Hagedorn [b], Torben Harz [a], Christian Fölsch [a,c], Bernd A. Ishaque [a,c], Markus Rickert [a,c], Alexander Jahnke [a]

[a] Laboratory of Biomechanics, Justus-Liebig-University Giessen, Klinikstrasse. 29, 35392 Giessen, Germany
[b] Department of Pathology, University Hospital Giessen and Marburg (UKGM), Langhansstrasse, 10, 35392 Giessen, Germany
[c] Department of Orthopaedics and Orthopaedic Surgery, University Hospital Giessen and Marburg (UKGM), Klinikstrasse 33, 35392 Giessen, Germany

ARTICLE INFO

Keywords:
Biomechanics
Endoprosthesis
Primary and secondary stability
Computational model
Data acquisition
Ultrasound

ABSTRACT

Aseptic loosening is a frequent cause for revision of endoprosthesis. X-ray examinations like Radio-Stereometry-Analysis (RSA) are among the most widely used in vivo methods for its detection. Nevertheless, this method is not used routinely because of bone marker and related radiation exposure. This work aims at creating a new in vivo concept to detect implant stability measuring micromotions without x-ray and to develop a corresponding algorithm. Based on the assumption of contactless measurement, the input parameters for the algorithm are the distances of each ultrasound sensor to the object (prosthesis and bone) and its position. First, the number of parameters necessary for a precise reconstruction and measurement of micromotions between objects had to be defined. Therefore, the algorithm has been tested with simulations of these parameters. Two experimental measurements, either using contact sensors or ultrasound, were used to prove the accuracy of the algorithm. Simulations indicate a high accuracy with three distances as initial parameters for each object. Contact measurements show precise representation of micromotion, and the contactless measurements show the possibility of detecting various materials with a high resolution. This work lays the foundations for non-invasive detection of micromotions between the implant-bone interface.

1. Introduction

Orthopedic surgery depends on improvements in technology, since further progress regarding clinical outcomes and longevity of joint replacements is required. Arthroplasties have made significant progress recently and are being referred to as the surgery of the century due to their improvement in quality of life [1]. Reconstruction of joint structures has a direct positive impact on patient health and mobility. The improvements showed positive results thanks to decreases in the percentage of revision and increase in life expectancy of an implant. Otherwise, an increasing number of joint replacements can be expected due to an aging society. Research into new diagnostic methods to assess the fixation of implants to detect loosening at an early stage appears useful despite improvements in endoprosthetic technology [2].

The issue is that diagnostic methods may not always clarify the bony anchorage of the endoprosthesis [3,4]. Primary stability is an important requirement for successful osseous integration of the implant [5,6]. Poor osseointegration and early aseptic loosening of the prosthesis were found correlated [7–9]. Therefore, primary stability analyses being indispensable to detecting aseptic loosening at an early stage have been the subject of research for several years [10].

Numerous in vitro studies address primary stability and have precisely shown the anchoring position and movements immediately after an implantation [3,4,11,12]. Many of these studies claim that primary stability has a direct correlation with the micromotions in the bone-implant interface. Therefore, estimating the micromovement between both objects could be essential for the osseointegration of the implant (secondary stability) [13–15].

Previous in vitro primary stability analyses could not adequately show biological and physiological processes following the implantation of the endoprosthesis. Since those processes could be relevant for loosening, different studies tried to describe stability in vivo. For example,

* Corresponding author.
E-mail address: Carlos.A.Fonseca-ulloa@med.uni-giessen.de (C.A. Fonseca Ulloa).

https://doi.org/10.1016/j.medengphy.2022.103932
Received 26 July 2022; Received in revised form 17 November 2022; Accepted 23 November 2022
1350-4533/

Bergmann developed a technically modified prosthesis, calculating actual forces and moments of the implant in vivo [16]. Other studies tried, with little modification in the stem, to detect and measure the changes in the resonance frequencies of the bone-prosthesis compound by different loosening states. [17,18]. These studies found that the mechanic information obtained through the difference in the resonance frequency is adequate for quantification of the primary and secondary stability of the implant. Furthermore, many studies are looking at modified dental prostheses, which found that the resonance of the implant is helpful for the stability status of the new tooth [19,20]. All these systems show a huge interest in the mechanical properties of the implant in vivo and therefore in the precise diagnosis of the primary and/or secondary stability. Since modification and positioning of sensors in the prosthesis are complex and expensive, none of these methods has been established as standard yet [16]. Although these in vivo technologies may be commercially available soon [21], the request for ways to detect loosening without modifying the implants was an important factor to be considered.

Ultrasound is already known to characterize several materials in a compound, and plenty of studies measure the movement and position of bones with ultrasound [22]. A very detailed example of bone reconstruction via ultrasound is the work of Hohlmann et al., which shows how precise an algorithm could be trained for bone segmentation [23].

An example of the characterization of prosthesis bone interface came from Hériveaux and colleagues who were able to describe with very detailed simulation and measurement methods the interface characteristics between both objects. This work concentrates and describes, in detail, the performance of the ultrasound reflection by changing the roughness of the implant and the thickness of the soft tissue [24]. All these works showed that it was possible to detect both materials (bone and implant) with an ultrasound system and that there are many factors (roughness, thickness of a soft tissue) to be considered for having an adequate reflection and reconstruction of the bone or the prosthesis with the ultrasound. Likewise, a dynamic measurement with ultrasound was also shown to be very accurate in the musculoskeletal system. All these systems which claim that the visibility and accuracy of the exact bone or prosthesis surface that they could be reliable methods for the process after implantation, although CT provides higher spatial resolution and susceptibility to artifacts.

The main goal of the present study was the development and validation of a new algorithm for an ultrasound-based diagnostic system for dynamic calculation of the stability of the prosthesis in vivo. The algorithm should approximate the bone and prosthesis to simple geometrical figures and determine how much information is essential for the measurement of the motion in the prosthesis bone interface. It should also be examined if a clinical ultrasound system might distinguish between the interface of endoprosthesis and bone as well as soft tissue, and whether the distances between the prosthesis and transducer or between bone and transducer could be measured with sufficient precision for motion measurements.

2. Materials and methods

First, the development of the functional requirements of the measurement system for clinical usability was investigated. The subject of investigation was to achieve a non-contact differentiation between the bone periosteum and the prosthesis surface without a prosthesis modification. For this purpose, the measurement system had to be applied externally to the skin without harming the patient. It should be possible to provide with this system a dynamic record of the movement between the prosthesis and the bone, at expected points of loosening of the prosthesis and under everyday loads. Soft tissue displacement of the skin and muscles remains a major limiting factor for the accurate detection of micromotion in the prosthesis bone interface [25]. Therefore, this new method aimed at enabling the recording of movement between bone and prosthesis as a motion relative to soft tissue displacement. The measurement described in this work will focus on hip implants with a range of distance between skin and bone of approximately 5 – 10 cm. The 10 cm value was chosen for the functional requirement, because it represents the worst-case clinical scenario corresponding to patients with adipose soft tissue and is in the range of actual computer tomographic measurements [26]. In order to minimize the input parameters and to try to simplify the measurement system, the model was based on a well-known geometry (circle) and mathematical derivate for a novel algorithm. Therefore, the algorithm needed three distances between each object and the sensor in order to reconstruct a circle as a representation for each object. Each sensor should measure at least two distances (to the bone and the implant) with high precision. The changing distance between both circles corresponded to the movements between the bone and the prosthesis. For this reason, Fig. 1a shows a transversal view of the system with simplified items. The "Z" component, representing the proximal-distal axis of the limb, could be determined by the measurement of different heights on the same object and therefore the algorithm is presented only with the movements in the X-Y plane.

2.1. Algorithm

The position of the prosthesis and bone circles were defined by the spatial position of their centers. The determination of the position was converted into a simple mathematical model Fig. 1b). To build these circles and define their spatial position, the algorithm needs a fixed distance between the sensor position and the radii of the bone and the prosthesis. These input values are the black highlighted variables R, alpha and beta. The values of these variables could be measured or determined on the routine radiographs taken directly after surgery. Sensors one to three were represented with S1, S2 and S3. The variables showed the location vectors and coordinates of the sensors in relation to a fixed reference point in space. These location vectors should be set before the measurement to align the system. The other three black variables Ra, Rb and Rc represented the measured minimal distance values between the objects and the sensors. The distance measured by the sensors is a totally unidirectional value and therefore the spatial position of the objects could not be calculated yet. Nevertheless, the values of each sensor showed a specific relationship with its own position and the distance to a specific point on the surface of the object. Therefore, the points on the object (O1–3) must be detected on the circumference of an imaginary circle with the radius Ra, Rb and Rc for the sensors S1, S2 and S3 respectively. Knowing the radius of the object and the angle between the sensors, the gap S1–2 and S2–3 (marked in green in Fig. 1b) between the measurement points could be calculated, since these stretches are the circular chords of the circles and defined by the following Eqs. (1) and (2).

$$S_{1-2} = 2 * R * \sin\frac{\alpha}{2} \tag{1}$$

$$S_{2-3} = 2 * R * \sin\frac{\beta}{2} \tag{2}$$

Then the blue colored sensor circles Fig. 1 were determined using the following three Eqs. (3), (4), and (5).

$$(O_{1x} - S_{1x})^2 + (O_{1y} - S_{1y})^2 = R_a^{\,2} \tag{3}$$

$$(O_{2x} - S_{2x})^2 + (O_{2y} - S_{2y})^2 = R_b^{\,2} \tag{4}$$

$$(O_{3x} - S_{3x})^2 + (O_{3y} - S_{3y})^2 = R_c^{\,2} \tag{5}$$

Since the three measurement points were approximately on a circular bone cross-section, the circle equation could be used to determine the center of the bone (Mk). Eqs. (8), (9), and (10) were then required.

$$(O_{1x} - M_{kx})^2 + (O_{1y} - M_{ky})^2 = R_k^{\,2} \tag{8}$$

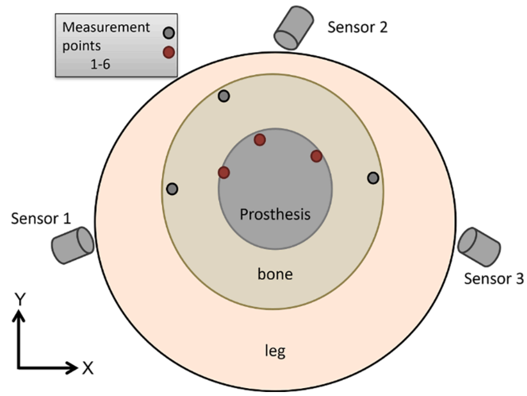

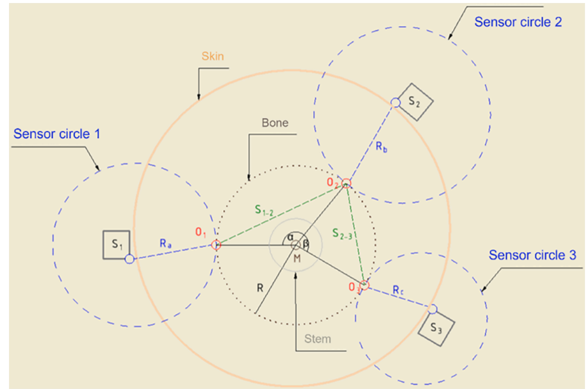

Fig. 1. a: Leg model based on circular shapes. Fig. 1b: Mathematical model of the in vivo concept for three different sensor positions.

$$(O_{2x} - M_{kx})^2 + (O_{2y} - M_{ky})^2 = R_k{}^2 \tag{9}$$

$$(O_{3x} - M_{kx})^2 + (O_{3y} - M_{ky})^2 = R_k{}^2 \tag{10}$$

Once the centers of the prosthesis and bone were defined, this procedure could be repeated for each measurement with regards to a specific height and time to obtain the whole motion curves of the prosthesis bone interfaces.

2.2. Simulation

The calculation of the relative movements ultimately corresponded to the difference in movement between the bone and prosthesis. For the investigation of feasibility, reproducibility, and errors of the algorithm, a simulation of the measured data was carried out. This simulation was implemented using LabVIEW® 2014 (National Instruments Corporation, Austin, USA). The LabVIEW® program simulated two cyclic motions in the X-Y plane at two different circle centers (measurement levels one and two) for the bone and the prosthesis. A total of four motions were analyzed (twice bone and twice prostheses). The radius for the prosthesis was set at 100 simulation units (SU) and for the bone at 300 SU. These SU were chosen to represent a relationship between prosthesis and bone of 1:3. This relationship allowed differentiation in the object representation and its movement in the LabVIEW® graphical interface. Three sensors were simulated so that for each measurement time, the algorithm consisted of six unidimensional distances between the sensor and the simulated circle. Originally, the radii, the position of the sensors, and the angles between the sensors were assigned and given to the algorithm as fixed input parameters. Then the cyclic movement of the prosthesis or the bone was simulated with a superposition of sine and cosine signals. The magnitude of the motion from the objects changes randomly. In a second simulation, an additional error was added to the already simulated measurement data. The error had a magnitude of $\pm1\%$ up to $\pm5\%$ of the measured data. This means that for each simulated sensor, an error of 1% up to 5% was randomly added to or subtracted from the original value. This corresponded to an inaccuracy of ±1 mm for a measurement distance of 100 mm between sensors and objects. These modifications were applied to the same simulated measured values to ensure high comparability between the data and the calculated results. In the end, the algorithm-calculated circle centers were compared with the simulated ones.

2.3. In vitro measurements

After the computer simulation model, the developed program was tested with a more realistic model in form of a small measuring set-up. Eighteen standardized measurements on five self-manufactured bone-prosthesis composite models were inspected. The measuring equipment was divided into four different components: The loading unit (1,2), the sensors (4), the bone-prosthesis composite (5a, 5b), and the sensor arrangement system (3) (Fig. 2).

For the first experimental setup 5 cylindrical objects (length: 27.53 cm diameter: 3.58 cm (radius = 17.92 mm)) of epoxy resin (RenCast ®, Huntsman advance materials GmbH, Bad Säckingen, Germany) were made (Fig. 4). In these cylinders, five different metal rods were inserted (length: 15.12 cm and average diameter: 1.92 cm (average radius = 5.96 mm)). The cylindrical epoxy resin acted as a simplified representation of a bone and the metal rods as a prosthesis.

The objects were made of different rod materials by keeping the same bone resin. The first (#1) and second (#2) measuring objects were made with steel rods. The first one had a flatter surface compared to the second one. The third (#3) and fourth (#4) objects were made of polished or rough aluminum rods (see Fig. 3). The fifth object (#5) was a smooth steel rod with a semicircular surface. The differences in the metal rods were used to create an artificial variability in the measurements and to simulate different implant-bone interface characteristics. All the rods were then rotated with a load of 25 Nm, and the resin bones were fixed at the other end, producing a relative movement at the interface of both objects.

2.4. Ultrasound measurements

After elaborate research on the current state of the art in clinical diagnostics, it was found that ultrasound sensors can differentiate between prosthesis, soft tissue, and bone using low-interference broadband amplifiers and frequency modulators. Regarding the hypothesis that ultrasound sensors could distinguish between prosthesis, bone and soft tissue, at first, an experimental setup was developed to test the differentiation between the two-materials epoxy resin and metal. Water served as transmission medium. An already established clinical system (Sonoline Adara, Siemens Healthcare GmbH, Erlangen, Germany) was used as ultrasound system with a 2 – 10 MHz broadband probe technology. A linear scanner transducer at 5 MHz or 7.5 MHz nominal frequency was used throughout the validation.

The accuracy of the ultrasound was tested in a static set-up in water (Fig. 4a) where the bone and the ultrasound transducer were 10 cm apart. The purpose of the setup is to analyze the reproducibility of the distinction of the two different materials (epoxy resin cylinder with an implanted metal rod) by means of ultrasound. For spatial reconstruction, the objects could be rotated around the longitudinal axis from 0° to 324° in 36° increments using a rotary knob.

By determining the minimum distances between the ultrasound sensor and the objects to be measured, the input parameter needed for the algorithm could be automatically provided (Fig. 4b). That means, the input parameters that were needed for the simulation and the in vitro contact measurements did not have to be considered for the measurement with the ultrasound system. It was important to establish

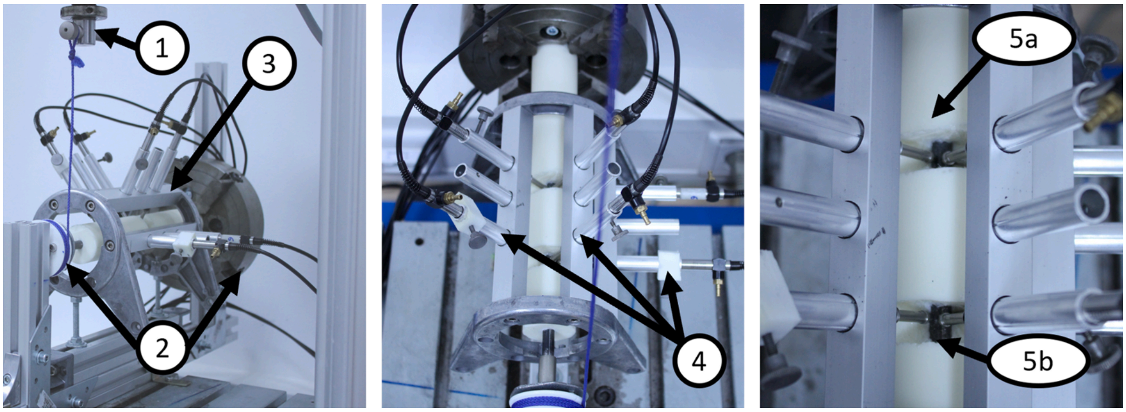

Fig. 2. Measurement system with tactile sensors.

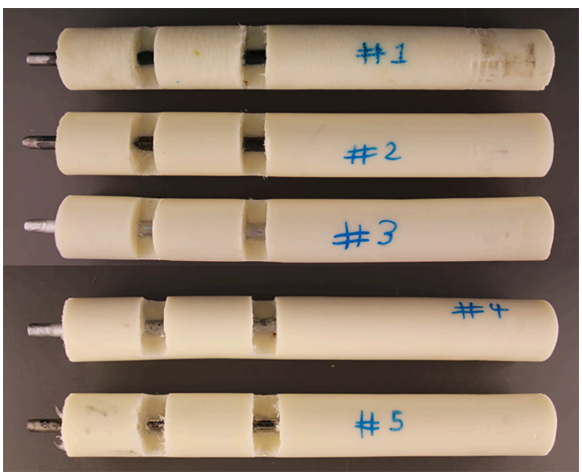

Fig. 3. Five measurement epoxy resin objects with different inserted metal rods.

the quality and accuracy of this system for this kind of in vivo measurement because the ultrasound system had not never been not used before for the calculation of relative movements at the prosthesis bone interface.

3. Results

3.1. Simulation

Table 1 lists the different simulated positions of the objects of three measurements. It also provides, the relative deviation between the locations in the X and Y plane of the object's center in simulation units calculated by the algorithm and the simulated object centers in SU.

The differences between one position and the next show the approximate course of the movement and its magnitude. Table 2 shows the interval between two positions (e.g., 1 >> 2), leading to the spatial movements of the prosthesis or the bone respectively.

Since the movements of the simulations were described without units or in SU, the relative deviations between the movements only had a limited significance. Therefore, the deviation of the movements was set in relation to the object radius. The last two columns of Table 2 show the comparison of percentage of motion differences, the object radius and the absolute difference in µm with the object having a realistic size of 4000 µm for a prosthesis radius and 10,000 µm for a bone radius.

The displayed curves in Fig. 5a and b show the comparison between the calculated and simulated values based on simulation of the transducers with built-in errors in their spatial position. Despite the large differences between calculated and simulated movements a point-to-point assignment of the simulated position to the calculated one is still possible. The positive and negative deviations as well as the size of the divergence are clearly shown in the data curve. The deviations were adjusted to the size of the measurement object (Table 3).

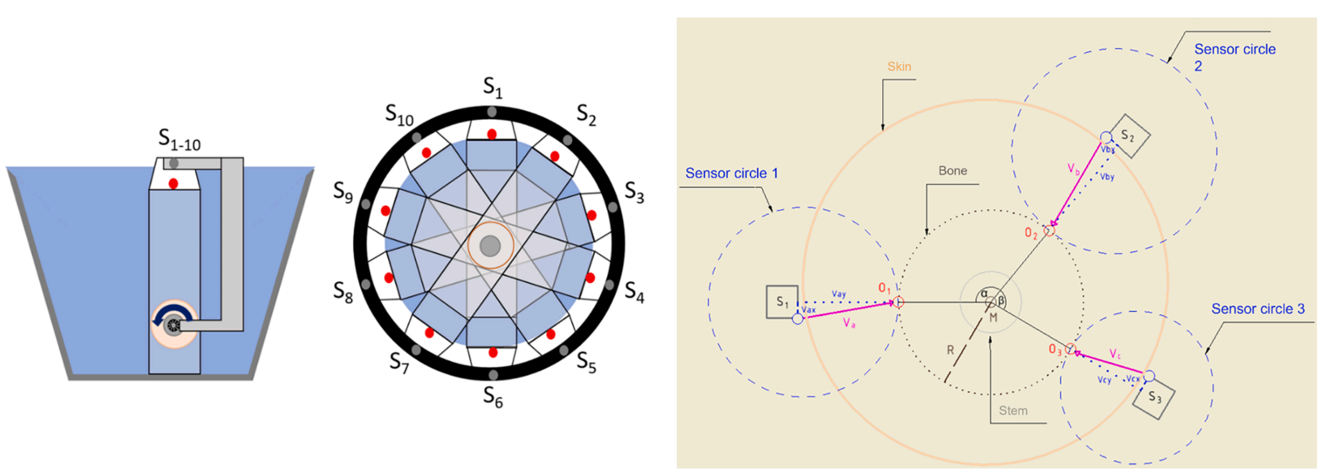

Fig. 4. a: Sketch of the contactless measurement system with ultrasound, with 10 possible sensors positions. Fig. 4b: Mathematical model of the ultrasound concept.

Table 1
Comparison between the simulated and calculated middle points of the simulated circle model in simulated units.

Stem ➔ Radius 100 [SU]							
Object	Position	Simulated middle point		Calculated middle point		Relative dev.	
		X [SU]	Y [SU]	X [SU]	Y [SU]	X	Y
#1	1	159.643	143.334	160.050	143.408	0.254%	0.052%
	2	127.023	143.334	127.132	143.450	0.086%	0.081%
#2	1	706.822	702.679	706.860	702.672	0.005%	0.001%
	2	703.959	708.318	704.318	708.354	0.051%	0.005%
	3	699.327	706.164	699.462	706.412	0.019%	0.035%
	4	699.327	699.194	699.548	699.226	0.032%	0.005%
	5	703.959	697.041	703.997	697.250	0.005%	0.030%
Bone ➔ Radius 300 [SU]							
Object	Position	Simulated middle point		Calculated middle point		Relative dev.	
		X [SU]	Y [SU]	X [SU]	Y [SU]	X	Y
# 1	1	147.684	143.334	148.067	143.650	0.259%	0.220%
	2	138.986	143.334	139.120	143.493	0.097%	0.111%
# 2	1	703.878	702.679	704.362	703.043	0.069%	0.052%
	2	703.051	704.032	703.019	704.161	0.004%	0.018%
	3	701.709	703.515	701.675	703.680	0.005%	0.023%
	4	701.709	701.843	702.077	702.068	0.052%	0.032%
	5	703.050	701.327	703.618	701.632	0.081%	0.043%

Table 2
Comparison between the simulated and calculated movements in simulated units and the relative and absolute deviation between them in μm.

Stem	Radius 100						Radius 4000 μm
Object	Positions	Simulated movement in [SU]		Calculated movement in [SU]		Relative deviation	Absolute deviation [μm]
		X	Y	X	Y		
# 3	1»2	1.14	−1.94	0.96	−2.07	0.03%	1.13
	2»3	2.99	−1.20	2.84	−1.31	0.09%	3.72
	3»4	3.70	0.00	3.86	0.22	0.17%	6.63
	4»5	2.99	1.20	3.08	1.32	0.13%	5.40
	5»6	1.14	1.94	1.12	1.82	0.12%	4.62
	6»7	−1.14	1.94	−1.33	1.90	0.07%	2.76
	7»8	−2.99	1.20	−2.84	1.27	0.11%	4.50
	8»9	−3.70	0.00	−4.05	−0.26	0.36%	14.57
	9»10	−2.99	−1.20	−2.94	−1.25	0.03%	1.11
Bone	Radius 300						Radius 10,000 μm
Object	Positions	Simulated movement in [SU]		Calculated movement in [SU]		Relative deviation	Absolute deviation [μm]
		X	Y	X	Y		
# 3	1»2	0.71	−5.75	0.63	−5.84	0.02%	2.46
	2»3	1.87	−3.56	1.75	−3.64	0.01%	0.65
	3»4	2.31	0.00	2.39	0.03	0.03%	2.88
	4»5	1.87	3.55	1.80	3.63	0.01%	1.21
	5»6	0.71	5.75	0.74	5.52	0.08%	7.59
	6»7	−0.71	5.75	−0.75	5.87	0.04%	3.99
	7»8	−1.87	3.56	−1.77	3.72	0.04%	3.59
	8»9	−2.31	0.00	−2.33	−0.36	0.02%	1.73
	9»10	−1.87	−3.55	−2.00	−3.55	0.02%	1.96

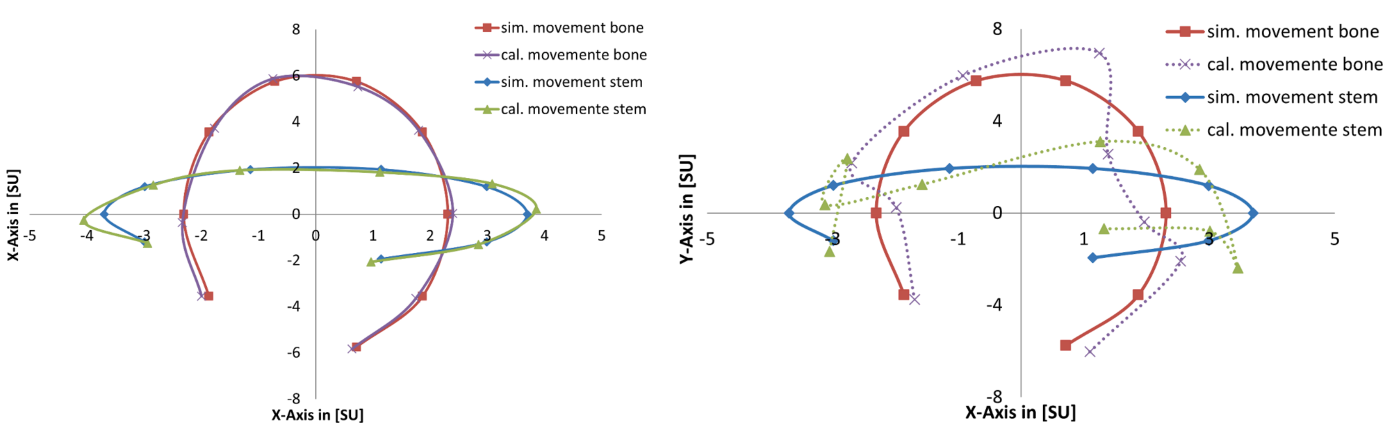

Fig. 5. a: Comparison between simulated and calculated movement. Fig. 5b: Comparison between simulated and calculated movement with built-in measurement error of 1–5% of the total movement.

Table 3
Relative movements between simulated bone with stem object in SU and movements deviation in µm.

Relative movements between bone and stem							
Object	Positions	Simulated movement in [SU]		Calculated movement in [SU]		Relative deviation	Absolute deviation [µm]
		X	Y	X	Y		
# 3	1»2	−21.91	−114.14	−16.27	−173.69	33.38%	58.23
	2»3	−57.42	−70.58	−35.51	−38.31	74.19%	38.75
	3»4	−70.95	−0.01	−72.74	82.80	35.63%	39.27
	4»5	−57.40	70.58	−67.68	9.54	33.09%	22.62
	5»6	−21.93	114.14	−8.87	107.59	7.66%	8.27
	6»7	21.93	114.17	32.20	149.24	23.85%	36.42
	7»8	57.40	70.57	35.08	58.07	34.08%	23.12
	8»9	70.95	0.01	44.30	−86.73	27.15%	26.44
	9»10	57.42	−70.58	65.43	−58.79	3.43%	3.02

3.2. In vitro measurements

The main feature of this measurement was the testing of the algorithm within an experimental setup. In this process the measurements were repeated three times. The reproducibility of the algorithm and the measurement system are shown in Fig. 6a. Additionally it was tested whether the algorithm can detect different material characteristics depending only on their movement. A representation of the different roughness of a steel rod can be seen in Fig. 6b.

The curves show small differences within object #4. The variations of the prosthesis are greater than those of the bone. The modeled prostheses are named with their actual properties (steel rod rough #1 and smooth #2) (Fig. 6b). The cyclic progression can be distinguished by the size of both measured objects. The prosthesis motion of both models was comparable, but the motions of the two bone models were different. That means the load transfer was different for both objects, although the prosthesis material was the same.

3.3. Ultrasound measurements

This measurement should prove whether conventional ultrasound equipment can detect different materials in an in vitro model in a similar setup as in vivo. To check the overall repeatability of the measurement chain itself all objects were divided into two groups (rod and cylinder bone). To prove the accuracy of the system the objects were reconstructed and the radius from both were compared to another measurement system (caliper: ± 50 µm). This comparison and the respective deviation are shown in table 4.

The standard deviation for both objects was very similar to the accuracy values of the caliper. In this scenario the variation by the prosthesis was higher than in the bone model. Hence the values of 120 – 190 µm showed that it could be possible to detect micromotions in this range.

Table 4
Comparison of the novel algorithm based reconstructed objects via ultrasound with the real object's dimension measure with a caliper.

	Rod	Bone
set value [mm]	5.96	17.92
mean [mm]	5.81	17.88
standard deviation [mm]	0.30	0.23
total deviation to set value [mm]	0.15	0.04
relative deviation to set value	2.50%	0.20%

4. Discussion

By improving treatment options in the field of endoprosthetics different groups examined how the implantation process could be optimized [27,16,28]. The results of these investigations led to an improvement of quality and longevity of endoprostheses [29]. Among others the improvements were achieved by combining different measurement methods such as the rotational measuring machines [11] or FEM simulations, where the initial parameters are defined by in vivo investigations [16]. Nevertheless, the high number of revisions, for example approximately 360.000 per year in Germany [29] indicates that further research is needed. Therefore, this study aims at closing a gap between in vivo and in vitro measurements combining existing methods by creating a possible solution for further in vivo diagnostics. The first milestone towards this solution was set by the conception of a novel method with the corresponding algorithm.

Considering two simulated measurements the accuracy of the algorithm in its current version was established. In the first simulation the simulated data were compared with the algorithm results. The object position determinations showed a relative deviation with a maximum of 0.30%. The movement differences between the two target positions have

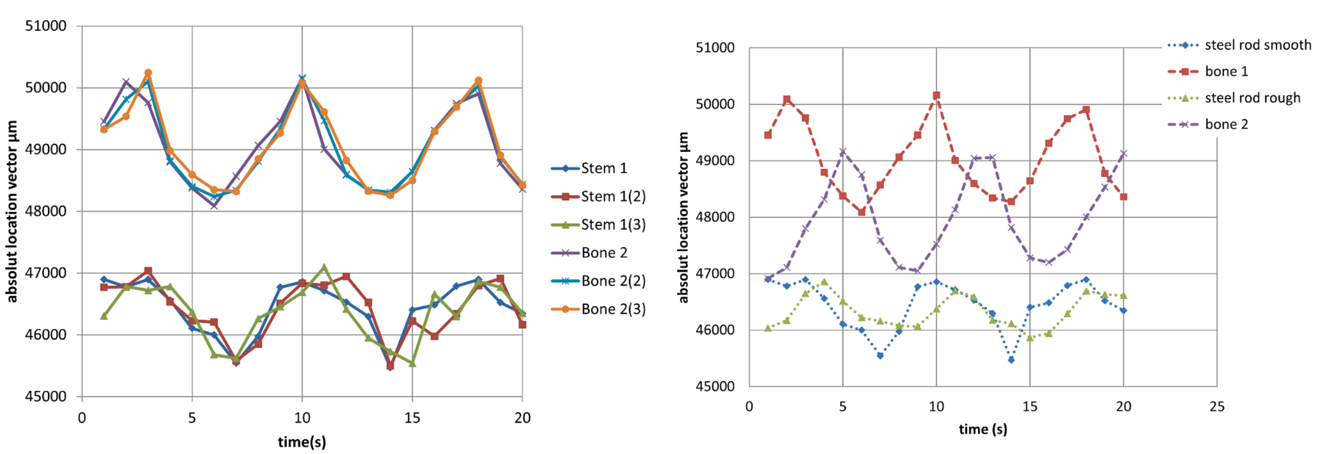

Fig. 6. a: Reproducibility of the object movement in the in vitro measurement with tactile sensors. Fig. 6b: Changes in the movements of the steel rods due to different roughness characteristics.

a mean deviation of 3.28 μm for the simulated bone and 5.96 μm for the prosthesis. The relative movement between each other is 4.53 μm on average. In the second simulation the deviations in the position determination were 7.36%, the movement differences with 13.17 μm and 12.24 μm and the relative movement with 28.46 μm significantly increased compared to the previous simulation.

Otherwise, the algorithm was used to measure relative motions between five bone/prosthesis test-specimens in an experimental measurement setup and the reproducibility related to the measurement repetitions was tested. The qualitative evaluation of the measurement results shows that the algorithm can represent the physical differences within the test objects. The reproducibility is given in four of the five measurement objects. Here the deviation was smaller than the relative movement by a factor of about ten.

At last, the algorithm was used to reconstruct and distinguish the two objects, cylinder bone and metal rod, by means of ultrasound information. In addition, these results were compared to another system to rank the general accuracy of the new method. The algorithm has shown an accuracy in the range of 0.2% to 1.6% or a reconstruction precision of the samples of 0.02 mm to 0.3 mm. Such or even higher accuracy is achieved by very few of the currently used in vivo systems, except for x-ray systems [30].

Compared to other in vitro measurement systems it should be noted that these relative movements of 300 μm are far from the precision of previously described systems such as Jahnke et al. with 0.1 μm [3] or Westphal et al. with 50 μm [31]. One of the most quoted studies claim that in order to assess good osseointegration it is necessary to record relative movements between 28 and 150 μm [9], although there is no clear limit for how much micromotions are allowed for a successful osseointegration. A review study reported a range of 30 and 750 μm ($\varnothing = 112$ μm) primary interface micromotions with secondary stability (osseointegration) [15]. Therefore, the technique used in this work has an accuracy between these ranges, which, however, is higher than the mean value for reported osseointegration and consequently this technique has limited accuracy for the full detection of primary stability be means of the measurement of micromotions. The accuracy of the ultrasound device as stated at 0.4 mm by the manufacturer is limited and crucial for the accuracy of the algorithm. Nevertheless, the results show that it is possible to visualize the difference between two materials (cylinder bone and metal rod) in water using ultrasound images. This was shown by the results of the accurate measurements for object reconstruction. The algorithm was able to reconstruct the cylinder bone cross-sections ($\varnothing = 17.92$ mm) as a circular shape at different measurement heights, with a mean radius of 17.88 mm and a standard deviation of $\pm$ 0.23 mm. Reconstruction of the metal rod ($\varnothing = 5.96$ mm) with a mean radius of 5.83 mm and a standard deviation of $\pm$ 0.30 mm at different measurement heights also proved possible, even considering different sound media. This high repeatability in the reconstruction of the bone by mathematical algorithms was also shown by Tarasevicius et al. in vitro and in vivo even on different materials [32].

This work contains numerous limitations, since it is a preliminary study to discover a simplified method for the detection and calculation of micromotion in the prosthesis bone interface. The model used to prove the algorithm is circular. This geometrical construct provides a simple mathematical identification of the movements, but it does not show the actual geometries of prosthesis and bones. Therefore, in future studies, the models must provide a larger number of input parameters to take more complex geometrical objects into account and also different kinds of prosthesis (cup, standard shafts, short stems, etc.). Nevertheless, the choice of an ultrasound system improves the ability for spatial measurement of the position of each object and therefore, the chance to reconstruct and define challenging geometrical objects.

Another form of proving the algorithm could be affected by means of inverse biomechanics. In the literature, many models have been shown to be very accurate in predicting load transfer and stability, including the characterization of bone and prosthetic materials. [33–35].

Another limiting factor consists in the fact that the algorithm has only been approved in a standard controlled protocol and a simple computer simulation. Before an in vivo measurement or a clinical trial could be done, the algorithm must be tested by means of studies of animal or human specimen and with different prostheses. Also, a comparison of the anchoring characteristic and movements with an established system [3,4,31] has to be made in order to prove the new method. Hériveaux et al. [24] show that with an ultrasound system it is possible to recognize different mechanics at the prosthesis bone interfaces. The combination and implementation of this knowledge in the new algorithm could be the key to the accuracy and sensitivity of the system.

Future studies are required to prove the precision of the ultrasound systems in the differentiation between real bone and prosthesis and the measurement of the movements between surfaces of the objects.

5. Conclusion

Development of this algorithm for the non-invasive determination of relative movements between the prosthesis bone interface in the human body has been advanced by this work. In addition, the foundations for a method for non-invasive calculation of relative motions has been predefined. The algorithm developed here can serve as a basis for creating new systems that can simplify the diagnosis of aseptic loosening. The authors are aware of the difficulty that it is a simplification of the stability problem and that more studies need to be performed in the future applying this algorithm to more realistic conditions (clinical studies, biomechanical simulations, etc.).

This computerized model is a first step in the advancement of an in vivo measurement of relative motion. This work identifies the basic requirements for a possible ultrasound-based diagnostic system. Such a system would fill a gap in measurement methodology found in the literature and could replace other measurement methods like x-rays methods, which could be harmful to the patient [36]. Further research in this field [17,18,37] indicates that such measurement systems being required for dynamic in vivo measurement of micromotions between prosthesis and bone could be beneficial for simplifying the diagnosis of prosthesis loosening and quality assessment of prosthesis in the future.

Funding

This research did receive a grant ("Graduiertenstipendium") from the Justus Liebig University in Giessen.

Ethical approval

Not required.

CRediT authorship contribution statement

Carlos A. Fonseca Ulloa: Conceptualization, Methodology, Software, Validation, Formal analysis, Investigation, Writing – original draft, Funding acquisition, Project administration. **Anja Seeger:** Software, Formal analysis, Writing – review & editing. **Frederike S. Hagedorn:** Visualization, Writing – review & editing. **Torben Harz:** Writing – review & editing. **Christian Fölsch:** Writing – review & editing. **Bernd A. Ishaque:** Writing – review & editing. **Markus Rickert:** Supervision, Funding acquisition, Writing – review & editing. **Alexander Jahnke:** Formal analysis, Conceptualization, Supervision, Project administration, Writing – review & editing.

Declaration of Competing Interest

None declared.

Acknowledgements

Not applicable.

References

[1] Learmonth ID, Young C, Rorabeck C. The operation of the century: total hip replacement. Lancet 2007;370(9597):1508–19. https://doi.org/10.1016/S0140-6736(07)60457-7.
[2] Clement ND, Biant LC, Breusch SJ. Total hip arthroplasty: to cement or not to cement the acetabular socket? A critical review of the literature. Arch Orthop Trauma Surg 2012;132(3):411–27. https://doi.org/10.1007/s00402-011-1422-2.
[3] Jahnke A, Fonseca Ulloa CA, Seeger JB, Rickert M, Jahnke GW, Ahmed GA, et al. Analysis of the elastic bending characteristics of cementless short hip stems considering the valgus alignment of the prosthetic stem. Clin Biomech 2018;52:49–56. https://doi.org/10.1016/j.clinbiomech.2018.01.006.
[4] Jahnke A, Bott CC, Fonseca Ulloa CA, Jahnke GW, Rickert M, Ishaque BA, et al. In vitro examination of the primary stability of three press-fit acetabular cups under consideration of two different bearing couples. Med Eng Phys 2019;67:49–54. https://doi.org/10.1016/j.medengphy.2019.03.008.
[5] Boy O, Hahn S, Kociemba E. Hüft-endoprothesen-erstimplantation. Düsseldorf; 2008.
[6] Okano T, Hagino H, Otsuka T, Teshima R, Yamamoto K, Hirano Y, et al. Measurement of periprosthetic bone mineral density by dual-energy x-ray absorptiometry is useful for estimating fixation between the bone and the prosthesis in an early stage. J Arthroplasty 2002;17(1):49–55. https://doi.org/10.1054/arth.2002.28729.
[7] Miron RJ, Bosshardt DD. OsteoMacs: key players around bone biomaterials. Biomaterials 2016;82:1–19. https://doi.org/10.1016/j.biomaterials.2015.12.017.
[8] Jakubowitz E. Experimentelle bestimmung der primären rotationsstabilität femoraler revisionendoprothesen in abhängigkeit von knöchernen substanzverlusten [Dissertation]. Heidelberg; 2007.
[9] Pilliar RM, Lee JM, Maniatopoulos C. Observations on the effect of movement on bone ingrowth into porous-surfaced implants. Clin Orthop Relat Res 1986;(208):108–13.
[10] Drosos GI, Touzopoulos P. Short stems in total hip replacement: evidence on primary stability according to the stem type. Hip Int 2019;29(2):118–27. https://doi.org/10.1177/1120700018811811.
[11] Görtz W, Nägerl UV, Nägerl H, Thomsen M. Spatial micromovements of uncemented femoral components after torsional loads. J Biomech Eng 2002;124(6):706–13. https://doi.org/10.1115/1.1517565.
[12] Thomsen M, Aldinger P, Görtz W, Lukoschek M, Lahmer A, Honl M, et al. Die bedeutung der fräsbahngenerierung für die roboterassistierte implantation von hüftendoprothesenschäften vergleichende experimentelle studie: hand- vs. roboterpräparation. Unfallchirurg 2001;104(8):692–9. https://doi.org/10.1007/s001130170070.
[13] Perona PG, Lawrence J, Paprosky WG, Patwardhan AG, Sartori M. Acetabular micromotion as a measure of initial implant stability in primary hip arthroplasty: an in vitro comparison of different methods of intial acetabular component fixation. J Arthroplasty 1992;7(4):537–47. https://doi.org/10.1016/S0883-5403(06)80076-8.
[14] Elliott B, Goswami T. Implant material properties and their role in micromotion and failure in total hip arthroplasty. Int J Mech Mater Des 2012;8(1):1–7. https://doi.org/10.1007/s10999-011-9172-4.
[15] Kohli N, Stoddart JC, van Arkel RJ. The limit of tolerable micromotion for implant osseointegration: a systematic review. Sci Rep 2021;11(1):1–11. https://doi.org/10.1038/s41598-021-90142-5.
[16] Bergmann G, Graichen F, Rohlmann A, Verdonschot N, van Lenthe GH. Frictional heating of total hip implants, part 1: measurements in patients. J Biomech 2001;34(4):421–8. https://doi.org/10.1016/S0021-9290(00)00188-3.
[17] Ruther C, Timm U, Ewald H, Mittelmeier W, Bader R, Schmelter R, et al. Current possibilities for detection of loosening of total hip replacements and how intelligent implants could improve diagnostic accuracy. In: Gueiral N, editor. Acoustic emission studies in hip arthroplasty - peak stress impact in vitro cemented prosthesis. editor. [sine loco]: IntechOpen; 2012.
[18] Bender T, Sass M, Bader R, Kluess D. P9.9 - SMART-HIP - entwicklung und auslegung eines sensorsystems für die messung der verankerung von implantaten. Tagungsband. AMA service GmbH, 49. Wunstorf, Germany: Von-Münchhausen-Str; 2015. p. 332–6. 31515- 2015.
[19] Miyashita M, Ogawa T, Naito H, Shibamoto A, Wang AS, Shobara K, et al. Evaluation of implant screw loosening by resonance frequency analysis with triaxial piezoelectric pick-up: in vitro model and in vivo animal study. Clin Oral Investig 2018;22(5):2129–34. https://doi.org/10.1007/s00784-018-2467-1.
[20] Nakashima Daisuke, Mikami Katsuhiro, Kikuchi Shunsuke, Nishikino Masaharu, Kitamura Toshiyuki, Hasegawa Noboru, et al. Laser resonance frequency analysis of pedicle screw stability: a cadaveric model bone study. J Orthopaedic Res® 2021;39(11):2474–84. https://doi.org/10.1002/jor.24983.
[21] Iyengar KP, Kariya AD, Botchu R, Jain VK, Vaishya R. Significant capabilities of SMART sensor technology and their applications for Industry 4.0 in trauma and orthopaedics. Sensors Int 2022;3:100163. https://doi.org/10.1016/j.sintl.2022.100163.
[22] Zheng M, Mohamadi A, Szabo T, Snyder B. Evaluation of in-vivo kinematics of cervical spines by co-registering dynamic ultrasound with MRI. In: Symposium IIU, editor. 2017 IEEE international ultrasonics symposium (IUS). editor. IEEE; 2017. p. 1–4. 06-09 Sept[Piscataway, NJ]2017.
[23] Hohlmann Benjamin, Glanz Jakob, Radermacher Klaus. Segmentation of the distal femur in ultrasound images. Curr Direct Biomed Eng 2020;6(1). https://doi.org/10.1515/cdbme-2020-0034.
[24] Hériveaux Y, Nguyen V-H, Brailovski V, Gorny C, Haïat G. Reflection of an ultrasonic wave on the bone-implant interface: effect of the roughness parameters. J Acoust Soc Am 2019;145(6):3370. https://doi.org/10.1121/1.5109668.
[25] Stagni R, Fantozzi S, Cappello A, Leardini A. Quantification of soft tissue artefact in motion analysis by combining 3D fluoroscopy and stereophotogrammetry: a study on two subjects. Clin Biomech 2005;20(3):320–9. https://doi.org/10.1016/j.clinbiomech.2004.11.012.
[26] Asvadi A, Dardenne G, Troccaz J, Burdin V. Bone surface reconstruction and clinical features estimation from sparse landmarks and statistical shape models: a feasibility study on the femur. Med Eng Phys 2021;95:30–8. https://doi.org/10.1016/j.medengphy.2021.07.005.
[27] Jahnke A, Ghandourah S, Fonseca Ulloa CA, Seeger JB, Rickert M, Ishaque BA, et al. Comparison of short stems versus straight hip stems: a biomechanical analysis of the primary torsional stability. J Biomech Eng 2020;142(12). https://doi.org/10.1115/1.4047659.
[28] Thomsen M, Aldinger P, Grtz W, Lahmer A, Honl M, Ngerl H, et al. Die bedeutung der frsbahngenerierung fr die roboterassistierte implantation von hftendoprothesenschften. Unfallchirurg 2001;104(8):692–9. https://doi.org/10.1007/s001130170070.
[29] Kärrholm J., Rogmark C., Nauclér E., Nåtman J., Vinblad J., Mohaddes M. et al. The Swedish hip arthroplasty register annual report 2019. The Swedish hip arthroplasty register; 2020.
[30] Khan MMK, Deshmukh SC, Theivendran K, Leslie LJ, Junaid S. A new diagnostic technique to detect early migration of joint prostheses. IEEE Access 2021;9:7021–32. https://doi.org/10.1109/ACCESS.2021.3049170.
[31] Westphal FM, Bishop N, Püschel K, Morlock MM. Biomechanics of a new short-stemmed uncemented hip prosthesis: an in-vitro study in human bone. HIP Int 2006;16(3):22–30. https://doi.org/10.1177/112070000601603S05. _suppl.
[32] Tarasevicius S, Skikas L, Mitraite D, Torii Y, Kesteris U, Wingstrand H. Sonography in total hip arthroplasty. Ultraschall Med 2007;28(5):475–8. https://doi.org/10.1055/s-2007-963287.
[33] Janssen D, Zwartelé RE, Doets HC, Verdonschot N. Computational assessment of press-fit acetabular implant fixation: the effect of implant design, interference fit, bone quality, and frictional properties. Proc Inst Mech Eng H 2010;224(1):67–75. https://doi.org/10.1243/09544119JEIM645.
[34] Mroz M, Rosenberg JL, Acevedo C, Kruzic JJ, Raeymaekers B, Naleway SE. Ultrasound freeze-casting of a biomimetic layered microstructure in epoxy-ceramic composite materials to increase strength and hardness. Materialia 2020;12:100754. https://doi.org/10.1016/j.mtla.2020.100754.
[35] Obata Y, Bale HA, Barnard HS, Parkinson DY, Alliston T, Acevedo C. Quantitative and qualitative bone imaging: a review of synchrotron radiation microtomography analysis in bone research. J Mech Behav Biomed Mater 2020;110:103887. https://doi.org/10.1016/j.jmbbm.2020.103887.
[36] Streit MR, Haeussler D, Bruckner T, Proctor T, Innmann MM, Merle C, et al. Early migration predicts aseptic loosening of cementless femoral stems: a long-term study. Clin Orthop Relat Res 2016;474(7):1697–706. https://doi.org/10.1007/s11999-016-4857-5.
[37] Alves SA, Polzehl J, Brisson NM, Bender A, Agres AN, Damm P, et al. Ground reaction forces and external hip joint moments predict in vivo hip contact forces during gait. J Biomech 2022;135:111037. https://doi.org/10.1016/j.jbiomech.2022.111037.